Selective Oxidation of Cyclohexane over Transition-Metal-Incorporated HMS in a Solvent-Free System

Jun Li,*,† Yong Shi,† Li Xu,† and Guanzhong Lu†,‡

Shanghai Institute of Technology, Shanghai 200235, China, and Laboratory for Advanced Materials, Research Institute of Industrial Catalysis, Research Institute of Industrial Catalysis, East China University of Science and Technology, Shanghai 200237, China

Mesostructure materials A-HMS (A = Ce, Ti, Co, Al, Cr, V, Zr) were synthesized with cetylamine as the structure director and tetraethyl orthosilicalite as the silica source. CeO_2/V-HMS and CeO_2/Al-HMS were prepared by dipping-calcination method. The materials were characterized by X-ray diffraction (XRD), UV−vis, Fourier transform infrared (FT-IR), N_2 adsorption−desorption, inductively coupled plasma−atomic emission spectroscopy (ICP-AES), transmission electron microscopy (TEM), and ^{27}Al magic angle spinning nuclear magnetic resonance (MAS NMR). The incorporated ions were mostly in the framework of the mesoporous materials, which were confirmed by the XRD, FT-IR, UV−vis, and ^{27}Al MAS NMR analyses. The solids obtained were employed as heterogeneous catalysts for the selective oxidation of cyclohexane with oxygen (O_2) as oxidant in a solvent-free system. The material CeO_2/V-HMS exhibited the highest activity with about 18% conversion of cyclohexane but 68% total selectivity to cyclohexanol and cyclohexanone. The performance of Al(40)-HMS is satisfying for nearly 10% conversion of cyclohexane and 93% total selectivity to the desired products. Also, Al(40)-HMS is efficient for its excellent recyclable property in the oxidation of cyclohexane.

1. Introduction

A great effort has been devoted to the research and development of new catalysts used in the oxidation of organic substrates for the most important industrial chemical reactions.[1] The oxidation of cyclohexane to cyclohexanol and cyclohexanone, which are intermediates in the production of adipic acid and caprolactam, are of great importance in the processes to manufacture nylon-6 and nylon-66 polymers.[2,3] However, for the modern industrial processes, the conversion of cyclohexane was usually lower than 5% in order to achieve high selectivity (about 80%) of cyclohexanone and cyclohexanol since the target products, cyclohexanone and cyclohexanol, are more active than the matrix. Moreover, in most cases, extreme reaction conditions such as high pressure and high temperature are required for the current industrial processes. So, it is necessary to find a new efficient catalytic system for the activation of cyclohexane. Catalytic materials often play an important role for an enhanced catalytic system. New mixed metal oxides were reported to be very efficient for selective oxidation of hydrocarbons;[4,5] the conversion of cyclohexane reached 25.8% with a selectivity of almost 90% to the main products cyclohexanol and cyclohexanone when the reaction mixture was magnetically stirred at 70 °C and with 1 atm of oxygen for 15 h.[4] Heterogeneous catalysts for hydrocarbon oxidation were reviewed,[6] and many details about this work can be found therein.

Since the discovery of silica-based mesoporous materials M41S in 1992,[7] the mesoporous materials have attracted considerable attention due to their high surface area, uniform pore size distribution, large pore size, and potential application in the fields of catalysis and separation. Many kinds of mesoporous materials, such as TUD-1,[8] Co/$MTiO_2$,[9] and HMS,[10] have been synthesized by using different templating agents. However, the pure silica mesoporous molecular sieves are poor in catalytic activity, so a number of transition metal (V, Bi, and Cr, etc.) incorporated mesoporous materials were synthesized and applied to catalytic oxidation of hydrocarbons.[11,12]

Transition-metal-incorporated MCM-41 were used as catalysts for the oxidation of cyclohexane, but organic solvents were usually added and *tert*-butyl hydroperoxide or hydrogen peroxide was applied as the oxidant, which may result in the contamination of the products and environmental problems.[11,12] Au/MCM-41[13] and Bi/MCM-41[12] were found to be very efficient for the conversion of cyclohexane in the solvent-free system, but the leaching of gold nanoparticles from the carrier is quite serious. It has been proved that a proper selection of preparation conditions is essential to obtain a homogeneous metal dispersion on the carrier, which in turn, generates highly active and selective catalysts toward oxidation reactions.[14] The mesoporous molecular sieve with wormhole framework structure denoted as HMS has many advantages, such as thicker framework walls, small crystallite size of primary particles, and complementary textural porosity. HMS can be synthesized by the sol−gel reaction with cheaper alkylamine as the template at room temperature,[15] and transition metal cations can be incorporated into the framework uniformly. Fe-HMS was synthesized successfully and used to catalyze the alkylation of benzene with benzyl chloride.[16] Our group found that Fe-containing HMS exhibited a good catalytic performance for the hydroxylation of phenol. Also, Co-AlPO-5,[17] Ce-AlPO,[18] Co-SBA,[19] Fe_2O_3−TiO_2,4 and metal-incorporated TUD-1 structure-type, mesoporous silicas[20] were found to be good candidates for the conversion of cyclohexane to cyclohexanone and cyclohexanol and left to be studied further. The kinetics and mechanism of cyclohexane oxidation were studied by many researchers in recent years,[21,22] which were useful for the development of powerful catalysts.

In many cases, the radical initiator, such as *tert*-butyl hydroperoxide, could decrease the induction period and increase the conversion of cyclohexane, but the initiator was not necessary for the selective oxidation of cyclohexane.[3,18,19] In the current work, we present a series of transition-metal-

* To whom correspondence should be addressed. Tel.: +86 021 64945006. E-mail: junliecust0967@sina.com.
† Shanghai Institute of Technology.
‡ East China University of Science and Technology.

10.1021/ie100092x
Published on Web 04/30/2010

incorporated HMS synthesized with an environmentally friendly cetylamine as template. HMS is a kind of mesoporous molecular sieve with wormhole framework structure. The metal-containing HMS were denoted as A-HMS (A = Ce, Ti, Co, Al, Cr, V, Zr). The CeO_2-loading A-HMS were also synthesized and were denoted as CeO_2/V-HMS and CeO_2/Al-HMS, respectively. The prepared samples were characterized by many physical−chemical methods. The catalytic performances of the synthesized catalysts for the selective oxidation of cyclohexane were studied in detail with molecular oxygen as an oxidant in a solvent-free system.

2. Experimental Section

2.1. Synthesis of the Catalytic Materials. The mesoporous molecular sieves A-HMS (A = Ce, Ti, Co, Al, Cr, V, Zr) were synthesized by a S^0I^0 assembly pathway. Tetraethyl orthosilicate (TEOS) and hexadecylamine (HAD) were used as a silicon source and template, respectively; the nitrates of cerium, cobalt, aluminum, chromium, and zirconium and ammonium metavanadate were used as the metal sources. In general, A-HMS can be synthesized according to the following procedure. The mixture solution containing TEOS, ethanol, and isopropyl alcohol (i-PrOH) was added dropwise to the mixture solution of alkylamine, the metal salt, ethanol (EtOH), and deionized water under vigorous stirring. The molar composition of this synthesis solution was SiO_2:AO_x:HAD:EtOH:i-PrOH: H_2O = 1:0.0167:0.27:6.5:1.0:36. After the synthesis solution was aged at 45 °C under stirring for 18 h, the solid formed was filtered, washed thoroughly with deionized water, dried at 100 °C, and calcined in air at 823 K for 10 h to obtain the A-HMS samples.

The resulting A-HMS sample (typically 0.8 g) was dispersed in 30 mL of isopropyl alcohol; then 23.2 mL of water solution (0.05 mol/L $Ce(NO_3)_3$) was added to achieve 20% loading. The above solution was dried while being stirred at ambient temperature and followed by calcination at 450 °C for 3 h at a heating rate of 2 °C to obtain CeO_2/Al-HMS and CeO_2/V-HMS.

2.2. Characterization of the Catalysts. The chemical−physical properties of the prepared materials were analyzed by powder X-ray diffraction method (XRD), N_2 adsorption/desorption, Fourier transform infrared (FT-IR) spectroscopy, UV−vis absorption spectra, inductively coupled plasma−atomic emission spectroscopy (ICP-AES), transmission electron microscopy (TEM), and solid-state ^{27}Al magic angle spinning nuclear magnetic resonance spectroscopy (MAS NMR).

X-ray diffraction analysis was performed on a Rigaku D/max-2400 diffractometer using Cu Kα radiation and a graphite monochromator. Diffuse reflectance spectrometry (DRS) UV−vis measurements were performed on a Varian Cary-500 spectrometer by using the diffuse reflectance technique in the range of 200−800 nm, and $BaSO_4$ was used as the reference. The Brunauer−Emmett−Teller (BET) surface areas and pore size distributions were calculated by using N_2 adsorption−desorption isotherms obtained on a Micromeritics ASAP 2020 sorptometer at 77K. FT-IR spectroscopy was obtained on a AVATAR 360 FT-IR spectrometer. The chemical compositions of the matrix gels and the calcinated samples were determined by ICP-AES. TEM images were obtained on a JEOL 2010 microscope operated at 200 kV. Solid-state^{27}Al MAS NMR measurements were performed using Bruke AVANCE III 500 NMR spectrometer at 130.3 MHz and a rotation rate of 5 kHz. Approximately 10000 scans were accumulated. Solid-state ^{27}Al chemical shifts were reported relative to 1.0 M $Al(NO_3)_3$ aqueous solution.

2.3. Activity Test of the Catalyst. The catalytic oxidations were carried out in a 25 mL stainless steel reactor equipped with a magnetic stirrer. In a typical reaction, cyclohexane (2 mL) was mixed with one of the prepared catalysts (10 mg) and then heated to the reaction temperature under a 0.5 MPa O_2 atmosphere. After reaction, the mixture of the reactant and products was cooled down and centrifuged to separate the catalyst. The analysis of the samples for the titled reaction was complicated and was discussed recently.[23] In this paper, the products were identified by gas chromatography−mass spectrometry (GC-MS; Agilent 6890N/5973N). Excess triphenylphosphine was added to the mixture in order to convert cyclohexyl hydroperoxide (CHHP) to cyclohexanol.[2] Cyclohexanone and cyclohexanol were analyzed quantitatively on a GC9790 (Wenling Corp. Ld., Shanghai, China) gas chromatograph equipped with a capillary column (30 m length, 0.32 mm i.d., and 0.25 μm film thickness) and a flame ionization detector (FID) using toluene as the internal standard. The conversion was calculated on the basis of the starting cyclohexane. Due to their decomposition in the condition of the chromatograph analysis, the CHHP and organic acids (probably including succinic acid, glutaric acid, valeric acid, caproic acid, and adipic acid) could not be analyzed by GC exactly.[24] In this paper, the CHHP was determined by iodometric titration[25] and the organic acids were analyzed by GC after being converted into their respective methyl ester as described earlier.[10]

Recycling tests were carried out by repeatedly using catalyst Al(40)-HMS in five consecutive reactions under 0.5 MPa O_2 at 140 °C for 4 h. After each reaction, the catalyst was separated by filtration from the reaction solution, washed with acetone, dried at 393 K for 10 h, and reused in the next run under the same reaction conditions.

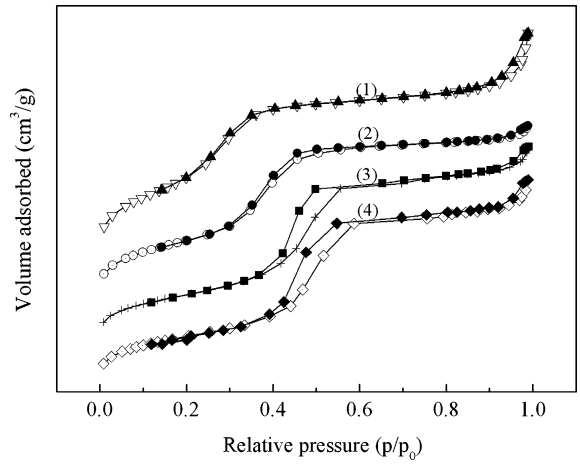

Figure 1. Nitrogen adsorption−desorption isotherms of the samples: (1) HMS, (2) Zr-HMS, (3) Al-HMS, and (4) Cr-HMS.

3. Results and Discussion

3.1. N_2 Adsorption−Desorption Isotherms. The N_2 adsorption−desorption isotherms corresponding to Barett−Joyner−Halenda (BJH) pore size distributions of the prepared samples are shown in Figures 1 and 2, respectively; the structural parameters are summarized in Table 1. The samples show the type-IV isotherms according to the IUPAC convention, indicating their mesoporors character, with a narrow pore distribution. The steep changes in volume adsorbed for P/P_0 = 0.25−0.4 or 0.35−0.55 indicate that the samples possess framework-confined mesopores.[10] H1 hysteresis loops also appear in the isotherms; that is to say, the samples are of mesoporous structure.[12] Compared with the pure HMS, the pore volumes of the A-HMS increases somewhat, while the specific surface areas become

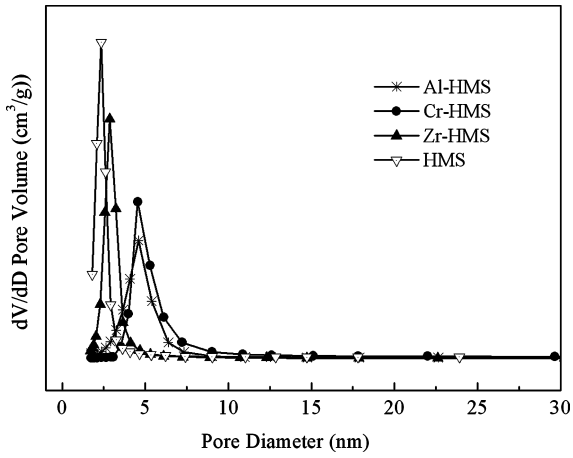

Figure 2. Pore size distribution of the synthesized samples.

smaller with the incorporation of the metal ions. Similar to the former report of our research group,[15] the present results above demonstrate the incorporation of the ions into the silicate framework lead to a modification of the HMS.

3.2. X-ray Diffraction Patterns. The low-angle powder XRD patterns of the prepared samples are shown in Figure 3. The samples prepared exhibit a well-resolved pattern with a sharp peak at $2\theta = 1.2-2.2°$ indexed to the (100) refractions of the A-HMS, which matches the character of a wormhole framework at low Bragg angle for the HMS[9] and in agreement with the previous work of our group.[15] With the incorporation of the trans-metal ions, the refraction peaks of the A-HMS shift to the low angle and the intensity of peaks decreases, as shown in Figure 3 and Table 1, which may be indicative of the incorporation of the ions into the framework of the silica mesoporous materials as the size of the incorporated cations are larger than Si^{4+}.[26] The Si/A ratios in the gels are similar to that in the products for the ratio of the Si/$A = 60$, while the difference of the Si/Al ratios between the matrix gel and the product become greater with the increase of Si/Al ratio in the starting gel, as shown in Table 1.

3.3. UV−Vis Diffuse Reflectance Spectrum. The UV−vis spectroscopy is known to be a very sensitive probe for an identification and characterization of transition-metal-ion coordination and its existence in the framework and/or in the extra framework position of metal-containing zeolites. UV−vis spectra of the A-HMS samples are presented in Figure 4. There are two absorption peaks at about 265 and 310 nm for the sample Ce-HMS. The absorption bands at about 265 nm are related to the charge-transfer transitions of O^{2-} to Ce(III) in the framework of the molecular sieve, and the bands at about 310 nm may be related to the charge-transfer transitions of O^{2-} to Ce(IV) in the extra framework.[27] So, the cerium species may present partly in the framework and partly as CeO_2 particles dispersed highly in the extra framework of the Ce-HMS. The absorbance peaks of the prepared Zr-HMS and Al-HMS are at about 210 and 220 nm, as shown in Figure 4, which correspond to the charge-transfer transitions of $O^{2-} \rightarrow$ Zr(IV) and the electronic transfer from oxygen to tetra-coordinated Al(III), respectively, while the absorbance peaks at ∼230 and 370 nm are related to the UV−vis spectra of ZrO_2 and Al_2O_3,[28] which are not found in the present spectra. There are two distinct peaks at ∼265 and ∼370 nm in the spectroscopy of the Cr-HMS; they are ascribed to the charge transfer of $O^{2-} \rightarrow Cr^{6+}$ (tetra-coordinated Cr^{6+} in the framework of Cr-HMS).[29] As for the spectrum of the V-HMS, there are two absorbance peaks at about 263 and 382 nm, which are associated with the electronic transfer of $O^{2-} \rightarrow$ V(IV) in the framework.[30] The above results are convincing proof that aluminum, zirconium, chromium, and vanadium were incorporated in the framework of HMS. The peak at ∼218 nm in the spectrum of Ti-HMS is an indication of $O^{2-} \rightarrow$ Ti(IV) in the framework, while the peak at ∼240 to ∼380 nm may be related to titania in the Ti-HMS.[31] The broad absorbance band between ∼360 and 580 nm for the Co-HMS suggests that a certain amount of tetrahedrally coordinated Co^{2+} is present in the framework of the prepared sample.[19,32]

3.4. FT-IR Spectra. The FT-IR absorption spectra of pure silica HMS and the synthesized A-HMS catalysts are presented in Figure 5a,b. In the range of the wavenumber, the samples all show three absorption peaks at ∼469, ∼804, and ∼1090 cm^{-1}, which are corresponding to the rocking, symmetric stretching, and asymmetric stretching of the intertetrahedral oxygen atoms in SiO_2 of the samples, respectively.[33] The vibration absorption band at about 1090 cm^{-1} is assigned to ν_{as}(Si−O−Si), while the wavenumbers of the absorption peaks at ∼1090 cm^{-1} for the A-HMS are 4−5 cm^{-1} lower than that of the pure HMS. The shift of the absorption peaks toward the lower wavenumber may be thought of as an indication of metal incorporating into the framework of silica tetrahedra.[26] The absorption peaks at ∼970 cm^{-1} may be assigned to the stretching vibrations of Si−OH in the framework of the samples and can be observed in the pure silica HMS. No new distinct peak is found in the metal-containing samples compared with the pure HMS except the differences in absorption intensity, as shown in Figure 5a. The peaks near 970 cm^{-1} may be related to Si−O−A bonds. The intensity of the peaks near 970 cm^{-1} decreases with an increase of the aluminum content in the framework of HMS, as demonstrated in Figure 5b. This indicates that Si−OH groups were changed or consumed and transformed to the Si−O−Al bonds.[34,35]

3.5. Surface Microstructure. The transmission electron microscopy image of the Al(40)-HMS sample reveals a typical wormhole mesopore structure, which is characteristic of HMS. The similar pattern of mesoporous silica materials were reported by Williams et al.[36] and Xu and co-workers.[37] As shown in Figure 6, a network of channels is regular in diameter, although a long-range packing order is absent. This is consistent with the above results of the XRD and N_2 adsorption−desorption measurements.

3.6. Solid-State ^{27}Al MAS NMR Measurements. The samples Al(60)-HMS, Al(40)-HM, and Al(20)-HMS were further characterized by ^{27}Al MAS NMR spectroscopy to probe the coordination of Al atoms in the structures. The results were shown in Figure 7. The three samples all produced spectra with intense resonances at ∼53 ppm and weak resonances at ∼−0.5 ppm. The signals at ∼53 ppm were assigned to four-coordinated structural aluminum species joined to four $Si(O)_4$ units in highly symmetrical tetrahedral coordination. The low-intensity signals centered around 0.5 ppm were characteristics of octahedrally coordinated aluminum species. The results presented here indicated that part of the aluminum introduced in the gel did not enter the silica framework during synthesis. The shape and position of the lines in the spectra are similar to those already reported.[38] The signal at ∼53 ppm became stronger with the increase of Al content, suggesting more four-coordinated species existed in the final materials. The presence of octahedrally coordinated Al species in this sample probably results from the low solubility of the precursor in the synthesis mixture.

3.7. Catalytic Behavior. It is desired to understand the influence of the incorporated ion types, content, and valence on the catalytic property, so the reactivity of the prepared

Table 1. Parameters of the Prepared Samples

samples	Si/A gel	Si/A after calcination	2θ (deg)	d_{100} (nm)	S_{BET} (m^2/g)	V_{meso} (cm^3/g)	pore size (nm)
HMS	∞	∞	2.12	4.17	950	1.08	3.3
Cr-HMS	60	62.4	1.48	5.97	685	0.89	4.5
Zr-HMS	60	62.0	1.70	5.20	705	0.83	4.2
Ce-HMS	60	62.1	1.29	6.85	692	0.80	5.3
Ti-HMS	60	62.2	1.89	4.67	789	0.91	3.8
Co-HMS	60	62.3	1.420	6.22	782	1.1	3.4
V-HMS	60	62.3	1.76	5.01	789	1.01	3.5
Al-HMS	60	62.2	1.420	6.22	759	0.89	4.6
Al(40)-HMS	40	43.0	1.33	6.65	653	0.89	5.3
Al(20)-HMS	20	22.7	1.22	7.24	538	0.74	6.00

materials has been tested comprehensively for the selective oxidation of cyclohexane under the condition of 0.5 MPa O_2 and 413 K without any solvent. The experiment results are presented in Table 2. It is shown that all samples exhibited catalytic activity with cyclohexanone and cyclohexanol as the major products. A certain amount of oxidative products was detected in the blank reaction with pure HMS as a catalyst, although the conversion of cyclohexane was much lower than that on other catalysts. The result may be thought of as the proof that the excellent performance of the metal-containing catalysts may arise from the presence of active matal sites in the catalysts A-HMS. The content of the CHHP is very high in the blank reaction system as compared with the results in the other systems with catalyst A-HMS, which is in line with earlier reports,[22,25] indicating that the doped metals in HMS were the key for the decomposition of CHHP. In many earlier reports about the selective oxidation of cyclohexane with solid catalysts, TBHP was added into the reaction system as free-radical initiator in order to accelerate the initiation step of the autooxidation process using molecular oxygen as oxidant.[25,3,11] The present results displayed in Table 2 show that the catalyst A-HMS is effective for the selective oxidation of cyclohexane using molecular oxygen as oxidant without extra free-radical initiator or cocatalyst. Similar observations were also found in refs 2, 12, and 18.

The catalyst Ce-HMS gives the highest total selectivity of cyclohexanone, cyclohexanol, and CHHP, while the synthesized Co-HMS shows the best activity of all the A-HMS samples for the reaction. The behavior of the catalyst Zr-HMS was

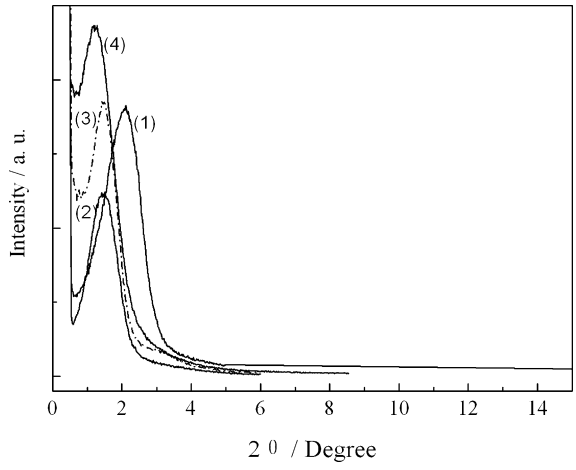

Figure 3. Low-angle powder XRD patterns of the synthesized samples: (1) HMS, (2) Al-HMS, (3) Co-HMS, and (4) Ce-HMS.

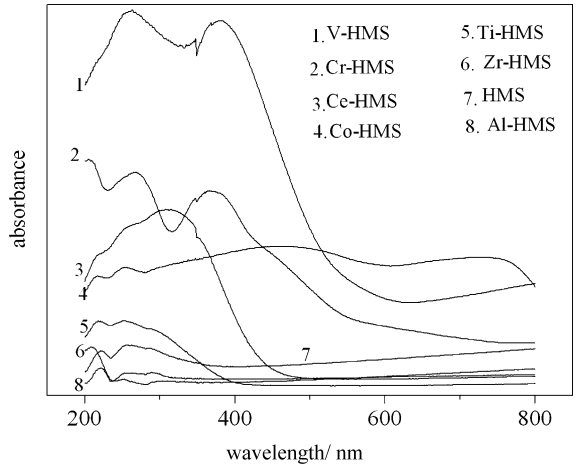

Figure 4. Diffusion reflectance UV−vis spectra of the synthesized samples.

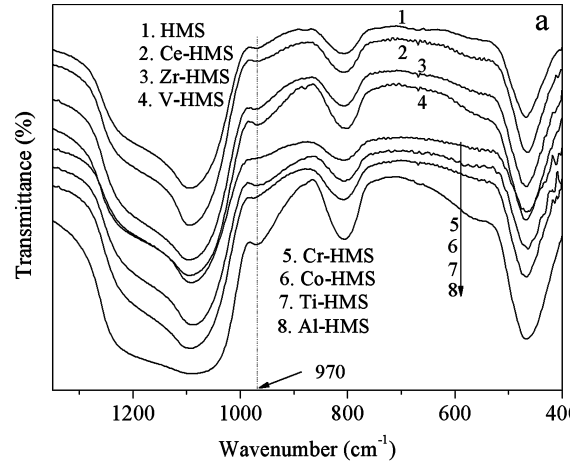

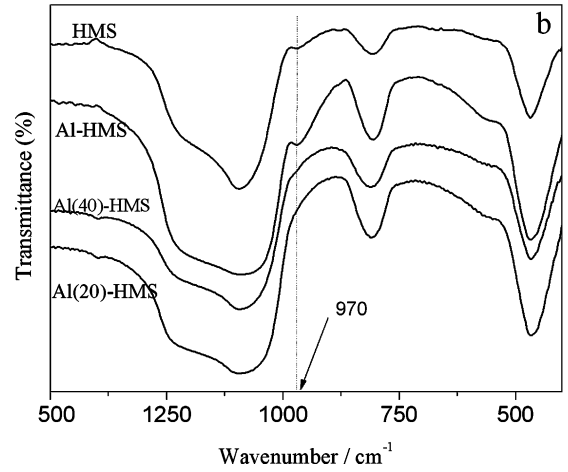

Figure 5. (a, b) FT-IR spectrum of the synthesized samples HMS, Al-HMS, Al(40)-HMS, and Al(20)-HMS.

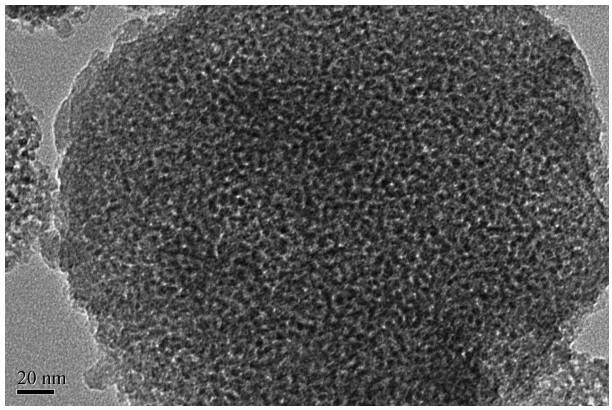

Figure 6. TEM image of the sample Al(40)-HMS.

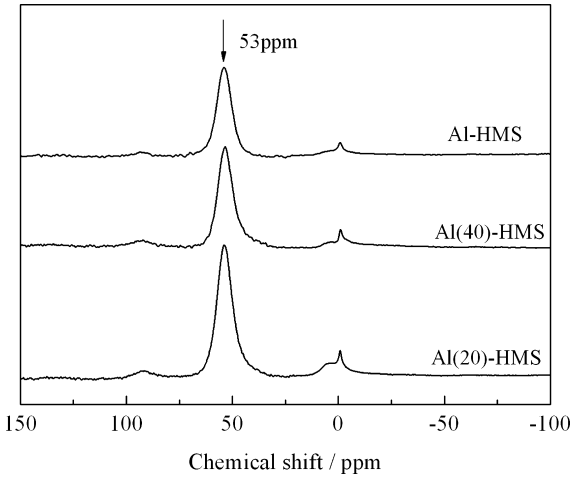

Figure 7. ^{27}Al MAS NMR spectra of the samples Al-HMS, Al(40)-HMS, and Al(20)-HMS.

unsatisfactory; the conversion of cyclohexane and the selectivity to the target products all are low over the catalyst Zr-HMS. The different activity and selectivity for the synthesized catalysts A-HMS may be plausibly attributed to the nature of the metal A used. The poor selectivity over Co-HMS may arise from the pore structure of the catalyst.[11]

Significant results were also obtained over the catalysts Cr-HMS, V-HMS, and Ti-HMS, as shown in the table. The result with Cr-HMS being used was comparable with that over chromium-containing hybrid mesoporous silica material using oxygen as oxidant in the solvent-free system,2 and better than the one over molecular sieve Cr-ZSM-5 3 under similar conditions. The total selectivities catalyzed by V-HMS or Ti-HMS all surpass 90%, while silica-supported oxide nanoparticles TiO_2/SiO_2 and V_2O_5/SiO_2 could give a selectivity of 100% to cyclohexanone and cyclohexanol with TBHP as oxidation agent at 80 °C.1 The difference of the catalytic characteristics between the present catalysts and the silica-supported oxide nanoparticles may arise mainly from the oxidants used, but we believe that the catalysts V-HMS and Ti-HMS are worthy of further study for the selective oxidation of cyclohexane with oxygen as oxidant in the solvent-free system.

When the Al-HMS and Al(40)-HMS were used for the selective oxidation of cyclohexane, both higher conversion and better selectivity were obtained though the results were not perfect. These results may be ascribed to the higher acidity of the catalysts and the state of Al in the catalysts.[39,40] The four-coordinated Al bears noticeable ability for the activation of molecular oxygen.[40] The catalysts CeO_2/V-HMS and CeO_2/Al-HMS behave much better than the others in activity but poor in selectivity. The performance of the above two materials is obviously different from the report by Zhao[18] who used CeO_2 as catalyst for the similar reaction system and obtained much lower activity but higher total selectivity. The said difference may be ascribed to the interaction between cerium and the incorporated element vanadium or aluminum in the present catalysts, which makes a high dispersion of CeO_2 on V-HMS or Al-HMS. In contrast, the CeO_2 used by Zhao was bulk particle. The lower activity of the Al(20)-HMS may be related to its smaller specific area and disorder compared with others, as shown in Table 1. The above results indicate the presence of the incorporated ions in HMS plays an important role in the reactions.

The kinetic results over the catalyst Al(40)-HMS in the oxidation of cyclohexane are shown in Figure 8a−c, which were obtained under the condition of 0.5 MPa molecular oxygen and different temperatures for 4−10 h. It shows that the conversion of cyclohexane and the selectivity to cyclohexanol changed slightly, while cyclohexanol steadily transferred to cyclohexanone or other chemicals with increasing reaction time. In contrast, the selectivity to cyclohexanone fluctuated obviously with a maximum at 6 h under 150 and 170 °C and decreased distinctly after 8 h, indicating more cyclohexanone being oxidated deeply. The befitting reaction time was about 6 h, as shown in Figure 8a−c. The kinetic trends presented in the above figure panels are similar for the given three temperatures in the main. This result demonstrates the kinetic rules are almost the same for the three temperatures. The results depicted here are

Table 2. Catalytic Properties of the Prepared Catalysts[a]

		selectivity (%)					
catalyst	conversion (%)	-ol	-one	CHHP	others	(-ol) + (-one) + CHHP	-one/-ol
HMS	2.77	20.6	26.0	48.5	4.9	95.1	1.3
Cr-HMS	7.69	29.0	60.9	3.8	6.3	93.7	2.1
Co-HMS	11.37	31.8	47.9	1.2	19.1	80.9	1.5
Zr-HMS	8.40	29.8	46.1	9.7	14.4	85.6	1.5
Ce-HMS	8.30	31.7	61.4	3.9	3.0	97.0	1.9
Ti-HMS	9.04	27.8	48.3	14.1	9.8	90.2	1.7
V-HMS	9.34	32.1	60.3	0.7	6.9	93.1	1.9
Al-HMS	10.70	33.3	58.4	0.2	8.1	91.9	1.8
CeO_2/V-HMS	17.80	29.4	38.65	13.6	18.3	81.7	1.3
CeO_2/Al-HMS	15.40	29.8	41.1	12.9	17.2	82.8	1.4
Al(40)-HMS	9.95	34.9	57.9	3.5	3.7	96.3	1.7
Al(20)-HMS	6.86	30.8	48.1	9.8	11.3	88.7	1.6

[a] Reaction conditions: 2 mL of cyclohexane, 10 mg of catalyst, 0.5 MPa O_2, 413 K, and 4 h. Column headings: CHHP, cyclohexyl hydroperoxide; -ol, cyclohexanol; -one, cyclohexanone; others, including valeraldehyde, adipic acid, succinic acid, glutaric acid, valeric acid, caproic acid, and trace of methyl cyclohexane and amyl alcohol.

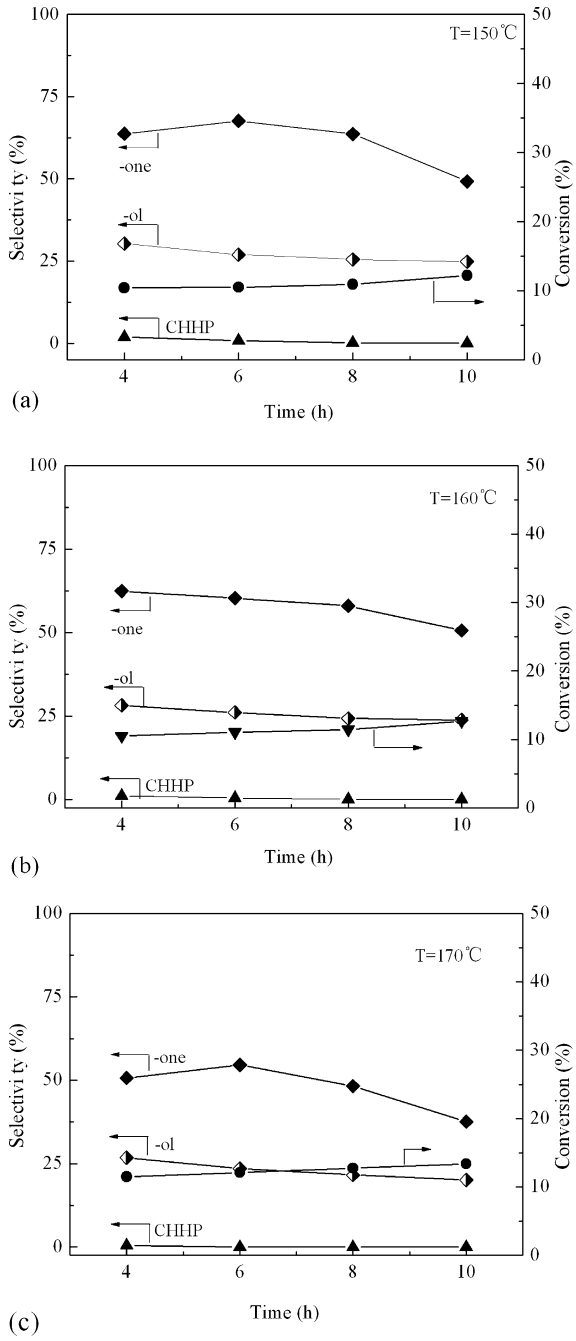

Figure 8. Catalytic activity of the catalyst Al(40)-HMS as a function of time under the condition of 0.5 MPa molecular oxygen: (a) 150, (b) 160, and (c) 170 °C for 4 h reaction.

comparable to that reported in literature,[2] where organic functionalized chromium-containing mesoporous silica materials were used as catalysts under solvent-free condition at different temperatures (100−160 °C) and air pressures (1.3−5.5 MPa) in the presence of small amounts (2 wt % cyclohexane) of free-radical initiator, TBHP. The content of CHHP in the mixture decreased gradually with the extension of reaction time and an increase of temperature, indicating that CHHP decomposed to the primary products such as cyclohexanol and cyclohexanone.

The effect of temperature on the product distribution is illustrated in Figure 9. With increasing reaction temperature in the range of 140−170 °C, the conversion of cyclohexane increased slightly, while the selectivity to cyclohexanol decreased stepwise due to their oxidation to cyclohexanone. There was a higher platform from 150 to 160 °C on the cure of the

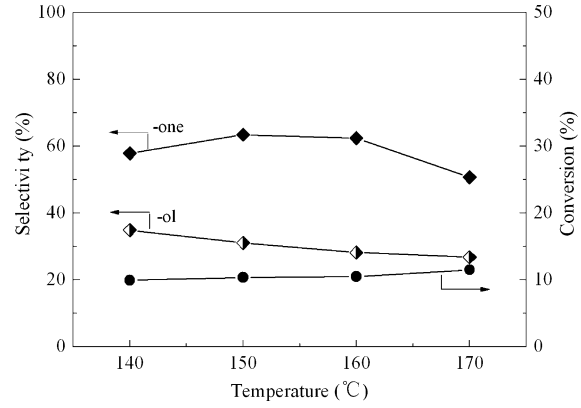

Figure 9. Influence of temperature on the performance of the catalyst Al(40)-HMS under the condition of 0.5 MPa molecular oxygen for 4 h reaction.

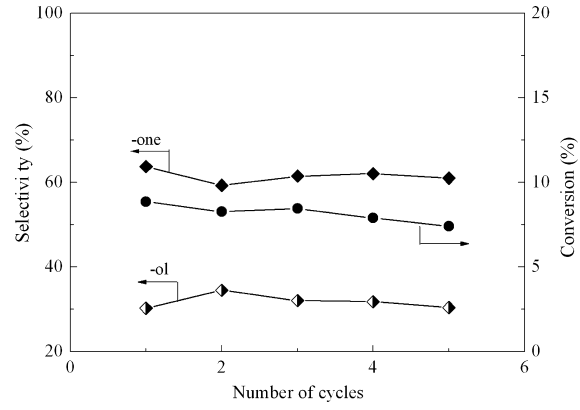

Figure 10. Recycling studies performed over the catalyst Al(40)-HMS under the condition of 0.5 MPa molecular oxygen and 150 °C for 4 h reaction.

selectivity to cyclohexanone. The cure went down significantly with the temperature above 160 °C due to the deep oxidation of cyclohexanone. Similar phenomenon was observed by Shylesh et al., who carried out the selective oxidation of cyclohexane with organic functionalized Cr-MCM-41 as catalyst.[2]

It was reported that cyclohexane was first converted to cyclohexyl hydroperoxide (ROOH).[41,42] ROOH rapidly decomposed to cyclohexanone and cyclohexanol, and cyclohexanol could be converted to cyclohexanone easily. In addition, cyclohexanone could be oxidated deeply. With the increase of reaction time and temperature, more ROOH and cyclohexanol transformed to cyclohexanone. Further oxidation of cyclohexanone was related to its concentration and reaction temperature; excessive time and temperature may result in lower selectivity to cyclohexanone, as displayed in Figure 8 and Figure 9.

The stability of the sample Al(40)-HMS was further explored. Five reaction runs were performed under the same condition. The results on the catalyst are shown in Figure 10. It can be seen that within the first three reaction cycles, the conversion of cyclohexane remains almost identical; after that, the activity of the catalyst falls a little, but no obvious change in Al content for the fresh and the recycled catalysts was detected by ICP-AES. The selectivity to both cyclohexanone and cyclohexanol remained almost the same for the recycling studies except the first run.

The above test confirms the recyclable property of the Al(40)-HMS for the selective oxidation of cyclohexane by O_2 in a solvent-free system. The results presented here are in accordance

with that displayed in the ref 3, where Co/ZSM-5 was used as the catalyst for the oxidation of cyclohexane by molecular oxygen.

Hot-filtration experiments were carried out with the catalyst Al(40)-HMS at 410 K under 0.5 MPa O_2. The reaction mixtures were filtered hot after reaction for 2 and 5 h in two separate experiments; the filtrates were then monitored for further reaction under stirring, but no increases in conversion were noted. The filtrates were also analyzed by ICP-AES; no aluminum was detected. These results suggest that Al(40)-HMS behaved as a heterogeneous catalyst, and the catalyzed reactions were truly heterogeneous.

4. Conclusions

A series of mesoporous materials A-HMS (A = Ce, Ti, Co, Al, Cr, V, Zr) were prepared successfully. Structural characterizations by various techniques revealed that the metals were incorporated into the framework of the HMS, but excessive incorporation of metal ions would make the mesoporous materials disordered with a significant decrease of specific area. All the prepared catalysts A-HMS were active for the oxidation of cyclohexane by oxygen in a solvent-free system. The prepared catalysts CeO_2/V-HMS and CeO_2/Al-HMS were very active with 17.8 and 15.4% conversion of cyclohexane, respectively, but the selectivity to the target products needs to be improved further. Of the metal-containing catalysts, Co-HMS gave the highest conversion, about 11% conversion of cyclohexane, while the total selectivity to cyclohexanone and cyclohexanol was only 79%. The behavior of the aluminum-containing Al(40)-HMS was appreciable; a conversion of about 10% was achieved with 92.8% total selectivity to cyclohexanonone and cyclohexanol. Moreover, the catalyst was stable in the reaction system. The befitting reaction temperature and time were about 150−160 °C and 6 h, respectively. The selective oxidation of cyclohexane over Al(40)-HMS with molecular oxygen as oxidant is environmentally friendly.

Acknowledgment

The authors acknowledge financial support from Shanghai Institute of Technology (KJ 20070-01) and the Committee of Science and Technology of Shanghai (06-JC-14095), China. We also thank Mr. Q.-Sh. Guo for his help in ^{27}Al MAS NMR measurement.

Literature Cited

(1) Susana, M.-M.; Yurgenis, H.; Olgioly, D.; Lindora, D.; Heinz, K. Catalytic properties of silica supported titanium, vanadium and niobium oxide nanoparticles towards the oxidation of saturated and unsaturated hydrocarbons. *J. Mol. Catal. A: Chem.* **2006**, *252*, 226–234.

(2) Shylesh, S.; Prinson, P. S.; Singh, A. Chromium-containing small pore mesoporous silicas: Synthesis, characterization and catalytic behavior in the liquid phase oxidation of cyclohexane. P. *Appl. Catal., A* **2007**, *318*, 128–136.

(3) Yuan, H.-X.; Xia, Q.-H.; Zhan, H.-J.; Lu, X.-H.; Su, K.-X. Catalytic oxidation of cyclohexane to cyclohexanone and cyclohexanol by oxygen in a solvent-free system over metal-containing ZSM-5 catalysts. *Appl. Catal., A* **2006**, *304*, 178–184.

(4) Perkias, N.; Wang, Y.; Koltypin, Y.; Gedanken, A.; Chandrasekaran, S. Mesoporous iron-titania catalyst for cyclohexane oxidation. *Chem. Commun. (Cambridge, U.K.)* **2001**, *11*, 988–989.

(5) Moises, A. C.; Vadim, V. G. Synthesis of catalytic materials on multiple length scales: From mesoporous to macroporous bulk mixed metal oxides for selective oxidation of hydrocarbons. *Catal. Today* **2005**, *99*, 137–142.

(6) Sheldon, R. A.; Wallau, M.; Arends, I. W. C. E.; Schuchardt, U. L. F. Heterogeneous catalysts for liquid-phase oxidations: philosophers' stones or Trojan horses. *Acc. Chem. Res.* **1998**, *31*, 485–493.

(7) Kresge, C. T.; Leonowicz, M. E.; Roth, W. J.; Vartuli, J. C.; Beck, J. S. Ordered mesoporous molecular sieves synthesized by a liquid-crystal template mechanism. *Nature* **1992**, *359*, 710–712.

(8) Anand, R.; Hamdy, M. S.; Gkourgkoulas, P.; Maschmeyer, Th.; Jansen, J. C.; Hanefeld, U. Liquid phase oxidation of cyclohexane over transition metal incorporated amorphous 3D-mesoporous silicates M-TUD-1 (M = Ti, Fe, Co and Cr). *Catal. Today* **2006**, *117*, 279–283.

(9) Yao, W.; Fang, H.; Ou, E.; Wang, J.; Yan, Zh. Highly efficient catalytic oxidation of cyclohexane over cobalt-doped mesoporous titania with anatase crystalline structure. *Catal. Commun.* **2006**, *7*, 387–390.

(10) Tanev, P. T.; Pinnavaia, T. J. A neutral templating route to mesoporous molecular sieves. *Science* **1995**, *267*, 865–867.

(11) Sakthivel, A.; Selvam, P. Mesoporous (Cr)MCM-41: A mild and efficient heterogeneous catalyst for selective oxidation of cyclohexane. *J. Catal.* **2002**, *211*, 134–143.

(12) Qian, G.; Ji, D.; Lu, G.-M.; Zhao, R.; Qi, Y.-X.; Suo, J.-S. Bismuth-containing MCM-41: Synthesis, characterization, and catalytic behavior in liquid-phase oxidation of cyclohexane. *J. Catal.* **2005**, *232*, 378–385.

(13) Lu, G.; Zhao, R.; Qian, G.; Qi, Y.; Wang, X.; Suo, A. Highly efficient catalyst Au/MCM-41 for selective oxidation cyclohexane using oxygen. *J. Catal. Lett.* **2004**, *97* (3−4), 115–118.

(14) Perkas, N.; Koltypin, Y.; Palchik, O.; Gedaken, A.; Chandrasekaran, S.; Chandrasekaran, S. Oxidation of cyclohexane with nanostructured amorphous catalysts under mild conditions. *Appl. Catal., A* **2001**, *209*, 125–130.

(15) Liu, H.; Lu, G. Z.; Guo, Y.; Guo, Y.; Wang, J. Study on the synthesis and the catalytic properties of Fe-HMS materials in the hydroxylation of phenol. *Microporous Mesoporous Mater.* **2008**, *108*, 56–64.

(16) Bachari, K.; Millet, J. M. M.; chouba, B. B.; Cherifi, O.; Figueras, F. Benzylation of benzene by benzyl chloride over iron mesoporous molecular sieves materials. *J. Catal.* **2004**, *221*, 55–61.

(17) Raja, R.; Sankar, G.; Thomas, J. M. Powerful redox molecular sieve catalysts for the selective oxidation of cyclohexane in air. *J. Am. Chem. Soc.* **1999**, *121*, 11926–11927.

(18) Zhao, R.; Wang, Y.; Guo, Y.; Guo, Y.; Liu, X.; Zhang, Z.; Wang, Y.; Zhan, W.; Lu, G. Z. A novel Ce/AlPO-5 catalyst for solvent-free liquid phase oxidation of cyclohexane by oxygen. *Green Chem.* **2006**, *8*, 459–466.

(19) Reddy, S. S.; Raju, B. D.; Padmasri, A. H.; Sai Prakash, P. K.; Rama Rao, K. S. Novel and efficient cobalt encapsulated SBA-15 catalysts for the selective oxidation of cyclohexane. *Catal. Today* **2009**, *141*, 61–65.

(20) Anand, R.; Hamdy, M. S.; Parton, R.; Maschmeyer, T.; Jansen, J. C.; Gläser, R.; Kapteijn, F.; Hanefeld, U. Metal-TUD-1 catalyzed aerobic oxidation of cyclohexane: A comparative study. *Aust. J. Chem.* **2009**, *62*, 360–365.

(21) Beale, A. M.; Grandjean, D.; Kornatowski, J.; Glatzel, P.; de Groot, F. M. F.; Weckhuysen, B. M. Unusual coordination behavior of Cr^{3+} in microporous aluminophosphates. *J. Phys. Chem. B* **2006**, *110*, 716–722.

(22) Hermans, I.; Peeters, J.; Jacobs, P. A. Origin of byproducts during the catalytic autoxidation of cyclohexane. *J. Phys. Chem. A* **2008**, *112*, 1747–1753.

(23) Anand, R.; Hamdy, M. S.; Parton, R.; Maschmeyer, T.; Jansen, J. C.; Hanefeld, U. Co-TUD-1 catalysed aerobic oxidation of cyclohexane. *Appl. Catal., A* **2009**, *355*, 78–82.

(24) Chen, J. D.; Sheldon, R. A. Selective oxidation of hydrocarbons with O_2 over chromium aluminophosphate-5 molecular-sieve. *J. Catal.* **1995**, *153*, 1–9.

(25) Zhou, L.; Xu, J.; Miao, H.; Wang, F.; Li, X. Catalytic oxidation of cyclohexane to cyclohexanol and cyclohexanone over Co_3O_4 nanocrystals with molecular oxygen. *Appl. Catal., A* **2005**, *292*, 223–228.

(26) Laha, S. C.; Mukherjee, P.; Sainkar, S. R.; Kumar, R. Cerium containing MCM-41-type mesoporous materials and their acidic and redox catalytic properties. *J. Catal.* **2002**, *207*, 213–223.

(27) Bensalem, A.; Muller, J. C.; Verduraz, F. B. From bulk CeO_2 to supported cerium-oxygen clusters: A diffuse reflectance approach. *J. Chem. Soc., Faraday Trans.* **1992**, *88*, 153–154.

(28) Chaudhari, K.; Bal, R.; Das, T. Kr.; Chandwadkar, A. S.; Srinivas, D.; Sivasanker, S. Electron spin resonance investigations on the location and reducibility of zirconium in mesoporous Zr-MCM-41 molecular sieves. *J. Phys. Chem. B* **2000**, *104*, 11066–11074.

(29) Samanta, S.; Malb, N. K.; Bhaumik, A. Mesoporous Cr-MCM-41: An efficient catalyst for selective oxidation of cycloalkanes. *J. Mol. Catal. A: Chem.* **2005**, *236*, 7–11.

(30) George, J.; Shylesh, S.; Singh, P. A. Vanadium-containing ordered mesoporous silicas: Synthesis, characterization and catalytic activity in the hydroxylation of biphenyl. *Appl. Catal., A* **2005**, *290* (1−2), 148–158.

(31) Corma, A. From microporous to mesoporous molecular sieve materials and their use in catalysis. *Chem. Rev.* **1997**, *97*, 2373–2420.

(32) Lou, Z.; Wang, R.; Sun, H.; Chen, Y.; Yang, Y. Direct synthesis of highly ordered Co-SBA-15 mesoporous materials by the pH-adjusting approach. *Microporous Mesoporous Mater.* **2008**, *110*, 347–354.

(33) Morey, M. S.; Brien, S. O.; Warz, S. S.; Stucky, G. D. Hydrothermal and postsynthesis surface modification of cubic, MCM-48, and ultralarge pore SBA-15 mesoporous silica with titanium. *Chem. Mater.* **2000**, *12*, 898–911.

(34) Wu, S.; Han, Y.; Zou, Y. C.; Song, J. W.; Zhao, L.; Di, Y.; Liu, S. Z.; Xiao, F. S. Synthesis of heteroatom substituted SBA-15 by the "pH-adjusting" method. *Chem. Mater.* **2004**, *16*, 486–492.

(35) Jang, M.; Park, J. K.; Shin, E. W. Lanthanum functionalized highly ordered mesoporous media: Implications of arsenate removal. *Microporous Mesoporous Mater.* **2004**, *75*, 159–168.

(36) Williams, T.; Beltramini, J.; Lu, G. Q. Effect of the preparation technique on the catalytic properties of mesoporous V-HMS for the oxidation of toluene. *Microporous Mesoporous Mater.* **2006**, *88*, 91–100.

(37) Chen, C.; Xu, J.; Zhang, Q.; Ma, H.; Miao, H.; Zhou, L. Direct synthesis of bifunctionalized hexagonal mesoporous silicas and its catalytic performance for aerobic oxidation of cyclohexane. *J. Phys. Chem. C* **2009**, *113*, 2855–2860.

(38) Bagshaw, S. A.; Jaenicke, S.; Khuan, C. G. Structure and properties of Al-MSU-S mesoporous catalysts: Structure modification with increasing Al content. *Ind. Eng. Chem. Res.* **2003**, *42*, 3989–4000.

(39) Araújo, R. S.; Azevedo, D. C. S.; Rodríguez-Castellón, E.; Jiménez-López, A.; Cavalcante, C. L., Jr. Al and Ti-containing mesoporous molecular sieves: Synthesis, characterization and redox activity in the anthracene oxidation. *J. Mol. Catal. A: Chem.* **2008**, *281* (1−2), 154–163l.

(40) Ono, T.; Nakamura, M.; Unno, K.; Oyun, A.; Ohnishi, J.; Kataoka, M.; Fujio, K. Partial oxidation of CH_4 over Al/silica catalysts using molecular oxygen. *J. Mol. Catal. A: Chem.* **2008**, *285* (1−2), 169–175.

(41) Tian, P.; Liu, Z.; Wu, Z.; Xu, L.; He, Y. Characterization of metal-containing molecular sieves and their catalytic properties in the selective oxidation of cyclohexane. *Catal. Today* **2004**, *93*−*95*, 735–742.

(42) Modén, B.; Zhan, B.-Z.; Dakka, J.; Santiesteban, J. G.; Iglesia, E. Kinetics and mechanism of cyclohexane oxidation on MnAPO-5 catalysts. *J. Catal.* **2006**, *239*, 390–401.

Received for review January 24, 2010
Revised manuscript received April 18, 2010
Accepted April 20, 2010

IE100092X